Excited-State Dynamics of $(SO_2)_m$ Clusters

T. E. Dermota, D. P. Hydutsky, N. J. Bianco, and A. W. Castleman, Jr.*

Departments of Chemistry and Physics, The Pennsylvania State University, University Park, Pennsylvania 16802

Received: May 13, 2005; In Final Form: July 1, 2005

A study of the excited-state dynamics of $(SO_2)_m$ clusters following excitation by ultrafast laser pulses in the range of 4.5 eV (coupled $^1A_2$, $^1B_1$ states) and 9 eV (F band) is presented. The findings for the coupled $^1A_2$ and $^1B_1$ states are in good agreement with published computational work[5] on the properties of these coupled states. A mechanism involving charge transfer to solvent is put forward as the source of the excited-state dynamics that follow the excitation of the SO_2 F band within $(SO_2)_{m+1}$ clusters with $m > 1$. The proposed CTTS mechanism is supported by calculations of the energetics of the process and the observed trends in the excited-state lifetimes that correlate very well with the calculated energies.

1. Introduction

Scientific interest in the much studied sulfur dioxide molecule stems in large measure from its presence as a pollutant in our atmosphere. Although some natural sources of SO_2 do exist, the bulk of the SO_2 in the atmosphere owes its origin to the combustion of sulfur-containing fossil fuels.[1] The ultimate fate of atmospheric SO_2 is oxidation to sulfuric acid, which may occur through more then one mechanism including gas-phase oxidation by OH or through solution-phase or heterogeneous processes when water and/or ice are present.[2]

Numerous studies of SO_2 can be found in the literature. A few notable examples are presented here but the extensive literature on the subject precludes the inclusion of a comprehensive list. Resonance enhanced multiphoton ionization experiments of the SO_2 monomer[3,4] and dimer[4] have resolved the energies of numerous electronic excited states and the accompanying vibrational levels. Computational investigations of the SO_2 potential energy surface[5−7] have elucidated details of SO_2 excited states including energies, coupling processes, and dissociation mechanisms. Experimental investigations from our laboratory have employed the pump−probe dynamics technique[8,9] to monitor the temporal evolution of electronic excited states in the SO_2 molecule[10] and clusters[11,12] on the ultrafast time scale. Cluster solvation was found to have substantial influences on the SO_2 electronic excited states under investigation. Therefore, detailed knowledge of molecular SO_2 is insufficient for an understanding of atmospheric chemistry where interaction with and solvation by other molecules is undoubtedly involved in the reactions of interest.

The objective of the SO_2 studies presented here is to gain further understanding of the influence of solvation/clustering on the electronic excited states of the SO_2 molecule. Thus even if the specific states under study are not major ones involved in atmospheric processes, elucidating how the potential energy surface of SO_2 is altered by molecular interactions further contributes toward an understanding of solution-phase and heterogeneous chemistry.

2. Experimental Methods

The experiments reported herein were performed using the well-established pump−probe technique[8,9] on an instrument consisting of an ultrafast laser system coupled to a reflection[13] time-of-flight mass spectrometer[14] equipped with a pulse-valve cluster source. The laser system[15] consists of a mode-locked Ti:sapphire oscillator (Spectra Physics Tsunami) that generates an 82 MHz pulse train and is pumped by a 10 W argon ion laser (Spectra Physics 2060). Pulse amplification is carried out by a regenerative Ti:sapphire amplifier pumped by the second harmonic of a 10 Hz Nd:YAG laser (Spectra Physics GCR 150-10) to produce pulses with an energy of 3 mJ/pulse and a temporal width of 100 fs. Experiments reported here were performed with the laser system tuned to ∼795, ∼810, and ∼825 nm to determine the influence of the wavelength on the excited-state dynamics. The fundamental output is frequency doubled by a BBO crystal and tripled by frequency mixing of the fundamental and doubled light to produce the probe and pump pulses, respectively. The exact wavelengths used are presented with the corresponding data. Clusters were generated by expansion of a 10% mixture of SO_2 in Ar backing gas (total pressure ∼3000 Torr) into an oil diffusion pumped high vacuum chamber (10^{-6} Torr) through a General Valve[16] pulse nozzle with a 0.254 mm diameter orifice. The ion signal generated by the probe pulse is detected by a two-plate MCP[17] detector. The signal from the MCP was acquired, averaged by a LeCroy 7200 oscilloscope,[18] and then transferred to a PC for analysis. The Delay line[19] that controlled the arrival time of the probe pulse and the oscilloscope are controlled by a PC using a program written in LabView.[20] All of the data reported here were taken at pump−probe delay times ranging from −2 to +50 ps, with the range from −2 to +2 ps having a data point every 100 fs and the range from +2 to +50 having a point every 500 fs. To acquire the data, the average of 20 laser shots was taken at each pump−probe delay time; this process was repeated five times and the results of the five passes though the pump−probe delay range were then averaged together, resulting in a total of 100 averages at each delay time. This procedure was employed to reduce the affect any fluctuations in the laser power or the cluster source may have on the data.

3. Results

3.1. TOF Mass Spectra. The mass spectrum shown in Figure 1 is typical of the signal obtained at the overlap of the pump

10.1021/jp052529u CCC: $30.25
Published on Web 08/27/2005

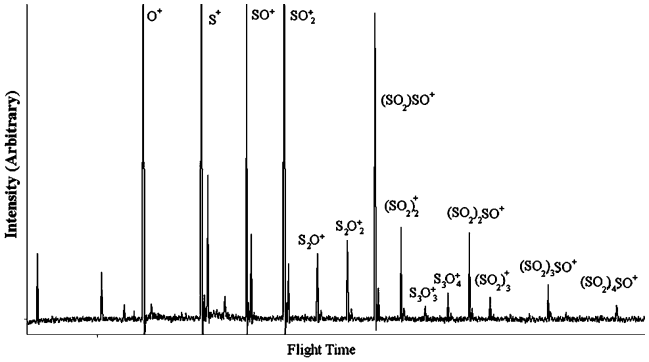

Figure 1. Typical TOF-MS of $(SO_2)_m$ clusters obtained at the temporal overlap of the pump and probe laser pulses.

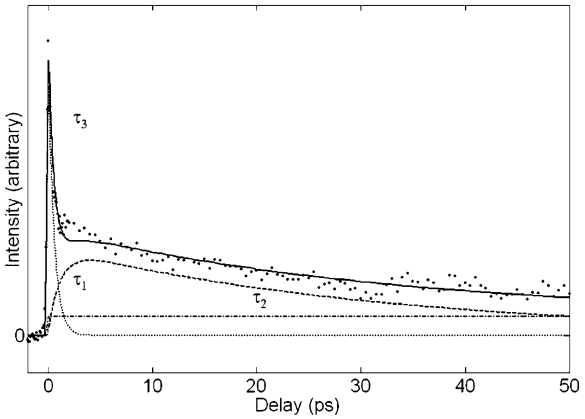

Figure 2. Pump−probe transient of the $(SO_2)SO^+$ ion signal showing the components of the temporal evolution. Pump: 265 nm, 0.06 mJ/pulse. Probe: 398 nm, 0.22 mJ/pulse.

and probe pulses. A few trends in the cluster distribution can be observed. For clusters consisting of m molecules, $(SO_2)_{m-1}SO^+$ is the dominant series in the cation mass spectra, which is the result of an oxygen atom being lost from each cluster. The loss of two and three oxygen atoms from clusters with $m = 2$ and 3 is also evident. It should be noted that the m/z 80 and m/z 144 species are labeled as being the result of three oxygen losses but could also be due to the loss of an S and an O leading to the formation of SO_3^+ and $(SO_2)SO_3^+$, respectively. However, the exact identity of the cluster products cannot be determined by the experimental methods employed here, although, as discussed later, the dynamical observations provide some information regarding the oxygen loss process. The monomer signal also indicates the presence of an oxygen atom loss as the SO^+ signal is larger in intensity than that of the SO_2^+ (truncated in Figure 1). In addition, S^+ and O^+ are observed at high laser pulse energies and at the temporal zero (as is the case in Figure 1). The nature of the oxygen loss channels and the formation of O^+ is discussed later in terms of the laser power dependence of the ion signal.

3.2. Fitting of Transient Data. A typical pump−probe transient for the SO_2 cluster system is shown in Figure 2 where the points represent the experimental data and the solid line represents the application of a fitting function to that data. Careful analysis of the SO_2 cluster transients revealed that they consist of three components. The three components can be described as a fast growth followed by a slow decay (dashed line), a fast decay (dotted line), and a constant intensity plateau (dot−dash line). The fitting function I that was used contains a term for each of the three components and is shown in eqs 1a−c. In eq 1a, a is the baseline signal intensity (subtracted from the data shown in Figure 2 to bring the baseline of the data to zero), c_1 is the intensity coefficient of the fast rise-slow decay, c_2 is the intensity of the fast decay, and c_p is the intensity of the plateau function (eq 1c).

$$I = a + c_1[I_2(t,\tau_2) - I_1(t,\tau_1)] + c_2[I_3(t,\tau_3)] + c_p[I_p(t)] \quad (1a)$$

The $I_n(t,\tau_n)$, function (eq 1b) was derived in ref 21 and published in the general form used here in ref 22. In this function, σ is the laser pulse width, τ_n is the time constant, t is the pump−probe delay time, and c is an adjustable parameter added to correct for any small variation in the assignment of the $t = 0$ step in the pump−probe transient.

$$I_n(t,\tau_n) = \left[1 - \mathrm{erf}\left\{\frac{\sigma}{2\tau_n} - \frac{t+c}{\sigma}\right\}\right] \exp\left\{\left(\frac{\sigma}{2\tau_n}\right)^2 - \frac{t+c}{\tau_n}\right\} \quad (1b)$$

The constant intensity plateau function (eq 1c) was derived by taking the limit of eq 1b as τ_n goes to infinity to produce a function that can account for the signal intensity in the experimental data that does not evolve on the time scale of the experiment.

$$I_n(t,\tau_n) \xrightarrow[\lim \tau \to \infty]{} I_p(t) = \left[1 - \mathrm{erf}\left\{-\frac{t+c}{\sigma}\right\}\right] \quad (1c)$$

The values of adjustable parameters in eqs 1a−c were determined by nonlinear regression fitting of the function to the experimental data using Oakdale engineering DataFit[23] software.

3.3. Probe Power Dependence of the Transient Data. The ionization potential (IP) of SO_2 is about 12.35 eV,[4] and the pump wavelengths used in these experiments lead to each pump photon having 4.5−4.7 eV of energy. As a result, both one and two photons of the pump may be absorbed by the SO_2 chromophore within the clusters, with three-photon absorption leading to ionization. Ionization of SO_2 following the absorption of one or two photons of the pump will require either three or one photon of the ∼3.1 eV probe, respectively. The energy diagram given in Figure 6 depicts the above-described process graphically and indicates the electronic excited states that are populated by the absorption of pump photons which will be discussed below.

To determine which of the two excited states populated by the pump produce each of the observed components, the probe laser power dependence of each component was determined. This was done by employing fitting of eq 1 to the data obtained at four probe pulse powers. Then, the intensity coefficient of each component of eq 1 was plotted as a function of the probe power and the data in the plot was fit to a power function. The exponent of the power function is the number of photons needed to produce the observed ion signal. Note that this procedure is often represented in the literature as a ln(I) vs ln(power) plot, which produces a straight line; however, the two methods are equivalent. A characteristic example of a power dependence plot is shown in Figure 3. The value of c_1 reaches its maximum at the second to lowest probe power used and remains constant when the power is increased. It is believed that at the higher probe laser powers, the ion signal remains at a constant maximum intensity because all of the excited-state population in the molecular beam that leads to the c_1 signal component is being ionized. The relatively low probe laser power needed to produce the maximum signal intensity indicates that the signal represented by c_1 does not require the absorption of a large number of probe photons. As a result, the c_1 component (the fast growth−slow decay component in Figure 2) must represent the dynamics of the excited-state populated by the absorption

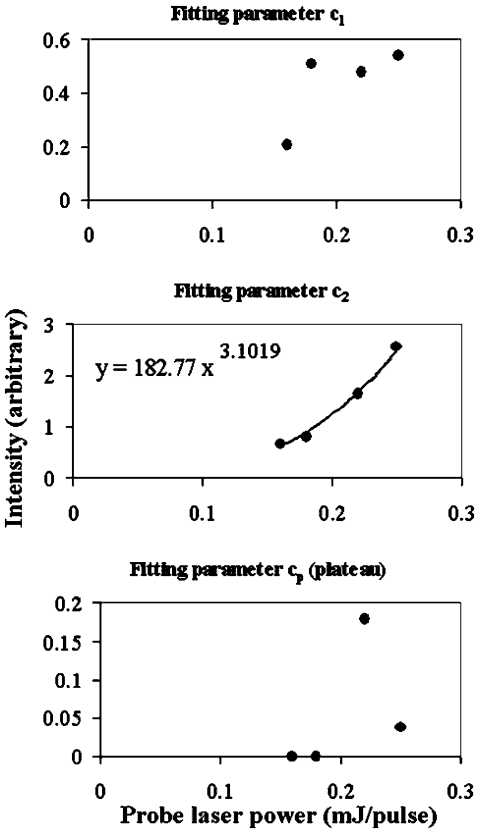

Figure 3. Probe power dependence of the three components of the transient data obtained from analysis of the $(SO_2)SO^+$ ion signal. Pump: 265 nm. Probe: 398 nm.

TABLE 1: Probe Power Dependence of the Ion Signal Transient Components Analyzed as Shown in Figure 3[a]

	photon order	
detected ion	c_1	c_2
	$m = 1$ series	
O^+	21	17
S^+	17	15
SO^+	saturated	saturated
SO_2^+	saturated	saturated
	$m = 2$ Series	
S_2O^+	saturated	1.9
$S_2O_2^+$	saturated	3.1
$(SO_2)SO^+$	saturated	3.1
$(SO_2)_2^+$	saturated	2.7
	$m = 3$ Series	
$(SO_2)_2SO^+$	saturated	3.6
	$m = 4$ Series	
$(SO_2)_3SO^+$	saturated	4.1
	$m = 5$ Series	
$(SO_2)_4SO^+$	saturated	3.9

[a] Pump: 265 nm. Probe: 398 nm.

of two pump photons, which produces an excitation less than one probe photon in energy below the ionization potential of SO_2. Fitting of the c_2 probe power dependence to a power function leads to an exponent of about 3, indicating that this component of the ion signal is the result of ionization from the one-photon pumped state. The intensity of the plateau, c_p, does not have a clear probe power dependence, making the assignment of its source difficult. Analysis of other clusters in the mass spectrum to determine the probe laser power dependence, shown in Table 1, produce comparable results, confirming the assignment of the components represented by c_1 and c_2.

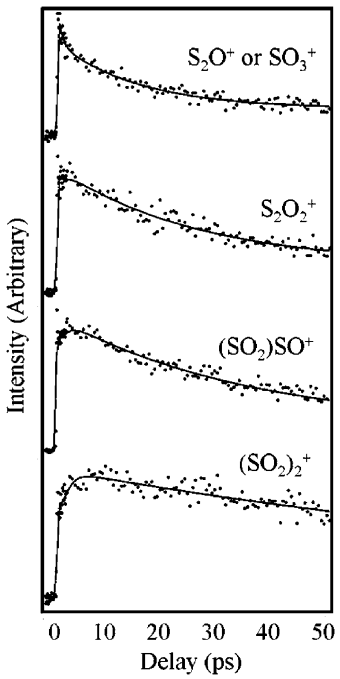

Figure 4. Pump−probe transients of the $m = 2$ cluster series. Pump: 264 nm, 0.05 mJ/pulse. Probe: 398 nm 0.11 mJ/pulse.

In addition to state assignment, the probe power study can be used to determine if the absorption of more probe photons than are needed to ionize the clusters is leading to the formation of cluster fragments. The values in Table 1 indicate that the oxygen loss process mentioned earlier from $m = 2$ clusters is not the result of the absorption of extra photons by the one photon pumped state represented by c_2 because each of the cluster fragments in the $m = 2$ series have the same value for the photon order within error. It should be noted that the fit to the power dependence of the m/z 80 cluster was particularly poor and as a result the value of 1.9 for the c_2 photon order is considered to be in agreement with the rest. The saturation of the c_1 signal component discussed above prevents the identification of the oxygen loss mechanism based on its power dependence. However, if probe photon absorption by the two-photon pumped state were responsible for the oxygen loss channel, the c_1 component would become more prominent relative to the c_2 component in the clusters that have lost oxygen atoms and become depleted in the $(SO_2)_2^+$ cluster. But, the opposite trend is observed, as can be seen in Figure 4. For the $m = 1$ series, the SO_2^+ and SO^+ signals show a saturation behavior to their power dependence, indicating that little probe power is needed to ionize these species compared to the clusters. However, the S^+ and O^+ require a large number of probe photons (the values in Table 1 for S^+ and O^+ may not be exact, but the finding that a large number of photons is needed is certainly correct). Therefore, these species are products of an excited ion-state process, as has been determined in previous investigations of the SO_2 mass spectrum.[4,12]

3.4. Transient Data Time Constants. Pump−probe transients of the $(SO_2)_{m-1}SO^+$ cluster series (data points) that have been fit to eq 1 are shown in Figure 5A. This set of data was obtained using a 0.05 mJ/pulse, 264 nm pump and a 0.11 mJ/pulse, 398 nm probe, which is considered to be a low probe power condition. Note that, with the exception of the SO^+, the c_2 component (growth and slow decay) is the dominant signal under the low probe power condition due to the need for only one photon to be absorbed for ionization (Figure 3) and that the time scale of the long decay increases with increasing cluster

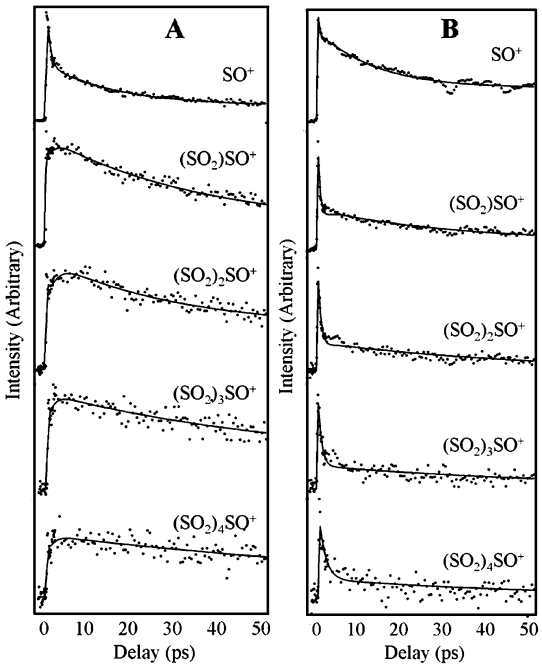

Figure 5. Pump−probe transients of the $(SO_2)_{m-1}SO^+$ cluster series. (A) Pump: 264 nm, 0.05 mJ/pulse. Probe: 398 nm 0.11 mJ/pulse. (B) Pump: 265 nm, 0.06 mJ/pulse. Probe: 398 nm, 0.22 mJ/pulse.

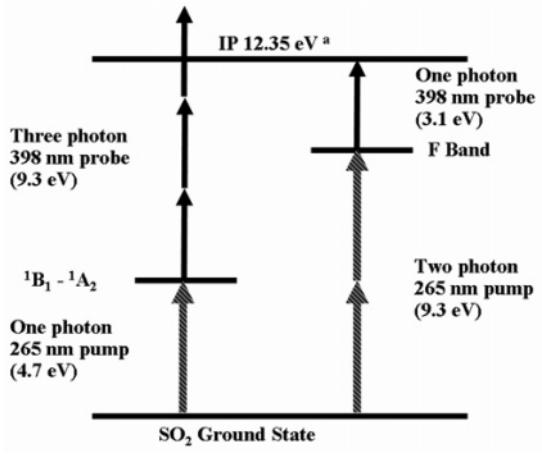

Figure 6. Energy level diagram depicting the generation of excited state populations in SO_2 by the absorption of one or two pump photons and ionization by probe photons.[4]

size. Figure 5B displays the pump−probe transients of the $(SO_2)_{m-1}SO^+$ cluster series taken under high probe power conditions using a 0.06 mJ/pulse, 265 nm pump and a 0.22 mJ/pulse, 398 nm probe. The higher probe energy results in an increase in the intensity of the c_1 (three photon) component relative to the c_2 component, which has reached its maximum intensity at a lower probe power.

The ability to adjust the intensities of components c_1 and c_2 relative to each other enabled the determination of the time constants of the overlapping decay component represented by c_2 and τ_3, and the growth represented by c_1 and τ_1, using the following procedure. Six sets of data taken under conditions similar to those for the data shown in Figure 5A were analyzed using eq 1 with the value of τ_3 fixed at 0.7 ps; all other parameters remained free to be adjusted in the optimization process. To determine the value of τ_3, six sets of data similar to that shown in Figure 5B were analyzed using eq 1, with τ_1 and τ_2 fixed at their average values from the low probe power data set. The average values of τ_1, τ_2, and τ_3 along with the standard deviation of the six values used (indicated as error bars) are shown in Table 2.

TABLE 2: Average Values of the Three Time Constants Obtained by Fitting of $(SO_2)_{m-1}SO^+$ Cluster Series Data Sets Obtained with an ∼265 nm Pump

	time constants (ps)		
detected ion {predicted neutral}	τ_1	τ_2	τ_3
SO^+ {$(SO_2)_2$}	0.7 ± 0.3	13.3 ± 3.0	0.6 ± 0.3
$(SO_2)SO^+$ {$(SO_2)_3$}	1.2 ± 0.2	32.8 ± 8.9	0.9 ± 0.4
$(SO_2)_2SO^+$ {$(SO_2)_4$}	1.3 ± 0.3	48.1 ± 16.2	1.1 ± 0.5
$(SO_2)_3SO^+$ {$(SO_2)_5$}	1.1 ± 0.2	65.0 ± 23.5	1.1 ± 0.3
$(SO_2)_4SO^+$ {$(SO_2)_6$}	1.5 ± 0.7	64.6 ± 49.0	1.1 ± 0.5

TABLE 3: Average Values of the Three Time Constants Obtained by Fitting of the $m = 2$ and 3 Cluster Series Data Sets Obtained with an ∼265 nm Pump, Indicating the Dependence of τ_2 on the Oxygen Loss Process

	time constants (ps)		
detected ion {predicted neutral}	τ_1	τ_2	τ_3
$m = 2$ Series			
S_2O^+ {$(SO_2)_3$}	0.8 ± 0.1	15.4 ± 5.7	0.7 ± 0.2
$S_2O_2^+$ {$(SO_2)_3$}	1.2 ± 0.6	21.6 ± 6.2	0.9 ± 0.4
$(SO_2)SO^+$ {$(SO_2)_3$}	1.2 ± 0.2	32.8 ± 8.9	0.9 ± 0.4
$(SO_2)_2^+$ {$(SO_2)_3$}	1.3 ± 0.3	73.7 ± 34.7	1.1 ± 0.6
$m = 3$ Series			
$S_3O_4^+$ {$(SO_2)_4$}	0.9 ± 0.2	35.4 ± 16.5	1.0 ± 0.6
$(SO_2)_2SO^+$ {$(SO_2)_4$}	1.3 ± 0.3	48.1 ± 16.2	1.1 ± 0.5
$(SO_2)_3^+$ {$(SO_2)_4$}	3.2 ± 4.3	76.2 ± 68.6	2.4 ± 1.9

TABLE 4: Average Values of τ_2 Obtained from the Analysis of Six Data Sets at Each of Three Pump Photon Energies[a]

m	pump (eV)	VDE (eV)	combined energy pump + VDE (eV)	time constant τ_2 (ps)
1	9.4	1.1	10.5	13.3 ± 3.0
	9.2		10.3	10.8 ± 4.3
2	9.4	2.8	12.1	32.8 ± 8.7
	9.2		11.9	17.3 ± 6.2
	9.0		11.8	10.1 ± 2.1
3	9.4	3.2	12.6	48.1 ± 16.1
	9.2		12.4	25.0 ± 12.9
	9.0		12.2	13.6 ± 3.4
4	9.4	3.5	12.9	65.0 ± 23.5
	9.2		12.7	31.9 ± 15.3
	9.0		12.6	16.8 ± 6.6
5	9.4	3.9	13.2	64.6 ± 49.1

[a] Also included are the vertical detachment energies (VDE) of $(SO_2)_m^-$ clusters as determined in ref 25.

In addition to the $(SO_2)_{m-1}SO^+$ cluster series, the clusters resulting from the oxygen loss by the $m = 2$ and 3 series were analyzed to investigate the source of the oxygen loss process(es). Each of the species in the $m = 2$ and 3 series exhibit the same qualitative behavior as the $(SO_2)_{m-1}SO^+$ series and have similar τ_1 and τ_3 values. However, the value of the slow decay time constant, τ_2, decreases with the cluster mass, as indicated by the values reported in Table 3.

3.5. Pump Wavelength Dependence of Time Constant, τ_2. To clarify the excited-state process responsible for τ_2 and to understand the influence that cluster size has on it, data were acquired at two pump wavelengths (∼270 nm and ∼275 nm) in addition to the ∼265 nm pump data presented thus far. The probe power was set fairly low to make c_1 the dominant component. As a result, τ_3 was not determined for pump wavelengths other than 265 nm. It was found that decreasing the pump energy decreased the value of τ_2 for the cluster sizes studied. The two-photon pump energies used and the average values of τ_2 for each cluster size m are shown in Table 4 along

with the vertical detachment energies of the $(SO_2)_m^-$ cluster anions, the significance of which is discussed shortly.

4. Discussion

4.1. Ionization Mechanism. As has been mentioned during the presentation of the mass spectrum in Figure 1, it is evident that some fragmentation or dissociation processes occur as a result of ionizing the neutral cluster distribution with the probe laser. Because the pump−probe experiment is performed on the neutral clusters, but the cations are the detected species, it is very important to identify the fragmentation and dissociation processes so the identity of the neutral species studied can be determined. It is known that SO_2 undergoes an oxygen loss process in the cation state. This process has been reported to occur with energies in the range of ∼3.5 eV above the cation ground state[4,26−28] and is therefore likely considering that, due to the high power density of the laser pulse, the absorption of additional probe photons is always possible when ultrafast laser pulses are used. This explains the loss of a single oxygen from each cluster leading to the observation of $(SO_2)_{m-1}SO^+$ as the dominant cluster series. However, the source of additional oxygen atom loss from the clusters is somewhat less clear. As indicated in Table 1, the probe power dependencies for all of the clusters in the $m = 2$ cluster series are the same, indicating that the loss of more than one oxygen atom is not due to the absorption of additional probe photons, as is the case for S^+. Also, each of the clusters from the $m = 2$ and $m = 3$ series have different values for the time constant τ_2, verifying that the process leading to the loss of additional oxygen atoms must be related to a neutral excited-state process. The observation of multiple oxygen losses from the clusters in both the pump−probe experiments and when direct ionization is employed presents a puzzling problem. This observation is addressed further in the discussion of F band dynamics.

Although the exact nature of the process that follows ionization of the clusters is not known, some assumptions are made to enable the discussion of the dynamics of the excited state. It is assumed that each detected cation cluster of the form $(SO_2)_{m-1}SO^+$ has undergone an oxygen atom loss and the evaporation of an SO_2 molecule during the ionization event (this process is independent of any oxygen loss or molecular evaporation discussed as a possible mechanism in the neutral state). As a result, each neutral cluster consists of m solvent molecules plus a chromophore molecule.

$$(SO_2)_{m+1} + h\nu \rightarrow (SO_2)_{m-1}SO^+ + SO_2 + O + e^-$$

The data table columns labeled "detected ion, predicted neutral" indicate the application of this assumption. As the data are interpreted in the following sections, it will become evident that although the assumption described here is not proven, it is self-consistent with the findings and their interpretation.

Excitation of the SO_2 chromophore within the clusters by the pump laser pulse leads to the formation of two populations of excited-state clusters within the molecular beam sample pulse. The coupled $^1A_2$ and $^1B_1$ states[5,29] are populated by the absorption of one photon, and the absorption band of SO_2 identified as the F band[30] is populated by the absorption of two pump photons (see Figure 6).

4.2. Interpretation of Time Constant, τ_3. The coupled $^1A_2$ and $^1B_1$ states are discussed first because the observed dynamics can be clearly explained on the basis of a detailed computational investigation of these coupled states. According to the findings of ref 5, the initial vertical excitation of the $^1B_1$ state is followed

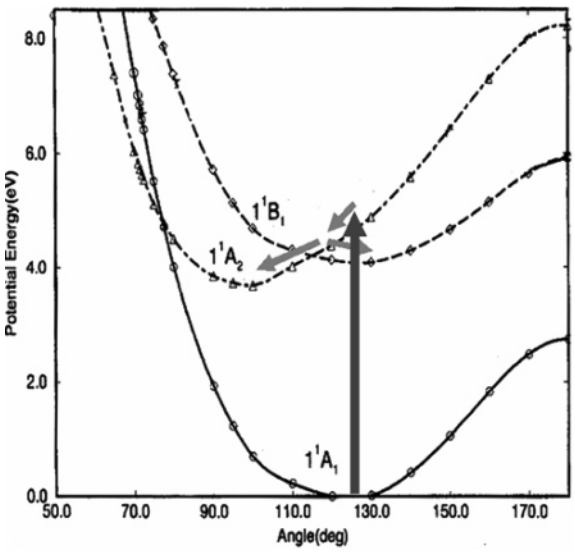

Figure 7. Graphical depiction of the excited-state population (light gray arrows) movement into the $^1B_1$ and $^1A_2$ potential well minima following pump photon absorption (gray arrow). SO_2 potential energy surface adapted from ref 7.

by movement of the excited-state wave packet from the $^1B_1$ state into the double wells that result from the crossing of the $^1A_2$ and $^1B_1$ states. This process is reported to proceed rapidly and be complete within 100 fs. The decay in the pump−probe transients represented by τ_3 is believed to be the result of the above-described process. This assignment is based on the finding of the power study presented in Figure 3 and Table 1, which indicate that c_2, the signal intensity coefficient associated with τ_3, requires the absorption of three probe photons to ionize the cluster. This is consistent with the energy needed to reach the IP of SO_2 from the $^1A_2$ and $^1B_1$ states. The ∼700 fs decay observed in the pump−probe experiment is likely to be a measurement of the time needed for the excited-state molecule to pass through the crossing between the initial $^1B_1$ excited state into the $^1A_2$- and $^1B_1$-state minima, as depicted in Figure 7. As can be seen from calculated potential energy surfaces[5−7] of this energy region, the potential energy-well minima of both the $^1A_2$ and $^1B_1$ states are not aligned well with the ground state. This indicates that the $^1A_2$- and $^1B_1$-state minima may be outside of the Franck−Condon region for the absorption of the probe laser pulse. The poor Franck−Condon overlap is particularly significant due to the need for a three-photon absorption to ionize the excited-state clusters. Therefore, ion signal is not observed once the transition has occurred. The value of τ_3 measured here is significantly greater than the <100 fs predicted,[5] but this is not entirely unexpected. It appears that the cluster environment is slowing the transition process. It seems reasonable to propose that, unlike the unperturbed conditions considered in the computational study, an ensemble of excited-state SO_2 molecules exist within the cluster population, each having a slightly different environment. For example, one excited-state molecule may be on the surface of its cluster and another may be more highly solvated within the cluster. For the signal in the pump−probe experiment to decay, all of the excited-state species must pass through the crossing of the $^1A_2$ and $^1B_1$ states, which requires that the molecules have the correct geometric parameters. This process is likely to be slowed by the excited-state molecules within the ensemble having a variety of geometries depending on each molecule's unique cluster environment. This argument is supported by the values of τ_3 reported in Table 2, which show a slight increase in lifetime with increasing cluster

size. A larger cluster would possess a larger number of possible environments of the excited-state molecules, increasing the time needed for the crossing to occur. Another factor to consider is that due to the pump wavelength of ~265 nm used in the experiments reported here, some excess energy is absorbed, putting the chromophore above the $^1A_2$ and $^1B_1$ crossing point, which is reported to occur with an excitation of around 300 nm[29,31] above the ground state. Additionally, as the clusters become larger, the difference in energy between the ground state and the $^1A_2$ and $^1B_1$ states may change due to solvation effects, leading to an alteration of the excess energy and possibly to the small increase in the measured value of τ_3.

4.3. Interpretation of Time Constants, τ_1, τ_2. Computational[6] and spectroscopic[41] investigations of the F band region of the SO_2 potential energy surface indicate that this energy region has a high density of states[6,41] with bound-state-like behavior.[41] However, because further details of this high-energy region of sulfur dioxide's excited-state potential energy surface are not well-known, cluster size trends and calculations based on standard enthalpies and energies from the literature are used to identify processes that may occur within the excited-state cluster. These findings are employed to develop a plausible explanation for the observed dynamics. Arguments are presented that discount some possible explanations for the observed results followed by a discussion of charge transfer to solvent, which is believed to be the operative mechanism leading to the observed dynamics.

4.3.1. Proposed Mechanisms. One possible process is that of caging, which requires the presence of a dissociative channel that is coupled to the F band. The energy region just above the F band has been studied by REMPI spectroscopy.[3] The study revealed that dissociative pathways are likely to exist in this region of the SO_2 potential energy surface. However, the spectroscopic findings for the F band[41] do not indicate the presence of a dissociative pathway. When caging is the operative mechanism, the transient data signal is often depleted near the zero delay time because the chromophore molecule cannot absorb the probe pulse shortly after the initial excitation due to the dissociation process. The signal then rises at later times when the dissociation process is stopped by molecules of the cluster that accommodate some of the energy of the dissociating fragments, allowing them to recombine into a bound molecule that can be ionized.[32] Two trends in the F band data disagree with an interpretation based on caging. First, the growth time constant τ_1 becomes somewhat slower with increasing cluster size (Table 2). Caging generally becomes faster and more efficient in larger clusters. Second, the slow decay component τ_2, which would represent evaporation in a caging mechanism, should become faster with increasing excitation energy but the opposite trend is observed here, as can be seen from the wavelength dependence of τ_2 presented in Table 4.

A second possible mechanism is that the excited state populated by the two photon pump is outside of the region where effective ionization by the probe laser can occur. In this mechanism, the initial excitation would be followed by a movement into the Franck−Condon region, resulting in increased signal intensity. However, upon excitation of the SO_2 molecule by the pump laser, the excited-state geometry is the same as that of the ground state. The geometry of the ground-state molecule is within the Franck−Condon region, as evidenced by its effective absorption of photons. As a result, one would expect the SO_2 molecule to be within the Franck−Condon region for ionization by the probe laser immediately after absorption of the two pump photons and therefore the rise represented by τ_1 is not likely to be the result of a Franck−Condon related process.

A third possible mechanism its that of a transition from the state initially populated by the two photon pump into a lower energy state with a better absorption cross section for the probe then the initial state. The improvement in absorption cross section would account for the rise represented as τ_1. A similar process has been observed in the case of $(SO_2)_m$ excited to the E-state surface.[11] Two processes were observed in the E-state work,[11] a dissociation of a SO_2 molecule on the E-state surface and an alternative relaxation pathway to a lower bound state. Relaxation to a lower bound state produced transient data with a two component decay. Each component had a different probe laser power dependence, indicating that the first component was the result of the initial excited state and the second component reflected movement to the lower-lying state. This type of behavior was not observed in the transient data presented here. Both the τ_1 and τ_2 components have the same probe laser power dependence, which is represented by c_1 (See Figure 3). In addition, the spectroscopic study of the F band region[41] indicated resolvable vibrational lines. If a fast transition or dissociation was occurring following excitation to the F band, vibrational lines would not be resolved.

4.3.2. Proposed Charge Transfer to Solvent Mechanism. The final and most likely explanation for the observed dynamics that follow the excitation of the SO_2 F band of a chromophore within $(SO_2)_m$ clusters involves the process of charge transfer to solvent (CTTS). According to observations from the literature that involve the study of CTTS in clusters[33−35] and in solution[36−39] (to reference a few of the many publications on the subject), the CTTS process proceeds by the following general mechanism. The chromophore is excited to a state somewhat above its ionization potential, resulting in the formation of a dipole-bound electron. Some of the energy of excitation is transferred to the solvent as the solvent is rearranging in response to the newly formed excited-state species and electron. This process results in the localization of the electron from the delocalized dipole-bound state on the time scale of ~1 ps or less.[33,36] Further solvation of the electron by the solvent leads to continued removal of energy from the electron on the time scale of 10's[33] to 100's[36] of picoseconds, possibly leading to solvent separation of the electron and the chromophore[36] when sufficient energy and solvent is available.

The proposed CTTS process is believed to manifest itself in the $(SO_2)_m$ data shown in Figure 5 in the following way. The initial state generated by absorption of the pump laser pulse is diffuse and, therefore, has a poor absorption cross-section for the probe so no ion signal is generated near the zero. As the electron becomes localized through solvent interactions, the absorption cross section improves and the signal intensity rises (τ_1). As the electron transfers its energy to the solvent, a relaxation process takes place that leads to the decrease in the signal intensity (τ_2).

4.3.3. Interpretation of Time Constant, τ_1. According to the CTTS mechanism, the values of τ_1 shown in Table 2 represent the time needed for the solvent molecules within the cluster to respond to the newly formed state. The observation that τ_1 increases with increasing cluster size supports the CTTS mechanism because more time is needed for the solvent to respond as the number of molecules in the cluster increases. In the case of photoinduced ion-pair formation in the HBr−water cluster system, which is a charge-transfer-like process, the solvent was found to respond to the newly formed ion pair on the time scale of 1 ps and the time increased with increasing

TABLE 5: Energy Calculation of the Charge-Transfer Process within an SO_2 Cluster[a]

$SO_2{\cdot}(SO_2)_m \rightarrow SO_2 + (SO_2)_m$	$+0.1$[b]
$SO_2 \rightarrow SO_2^+ + e^-$	$+12.35$[c]
$(SO_2)_m + e^- \rightarrow (SO_2)_m^-$	$-$VDE[d]
$SO_2^+ + (SO_2)_m^- \rightarrow SO_2^+{\cdot}(SO_2)_m^-$	$-A$
$SO_2{\cdot}(SO_2)_m \rightarrow SO_2^+{\cdot}(SO_2)_m^-$	$=$

[a] The VDE values for the cluster sizes studied are shown in Table 4. [b] Reference 24. [c] Reference 4. [d] Reference 25.

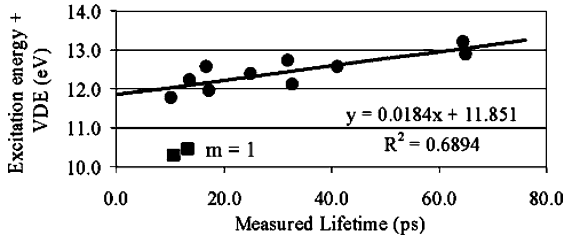

Figure 8. Linear plot of the correlation between the value of τ_2 and the combined excitation energy and VDE.

cluster size, as seen here.[42,43] Also, the ~1 ps value of τ_1 agrees well with other observations of this step in the CTTS process.[33,36]

4.3.4. Energetics of the CTTS Mechanism. The CTTS process requires the generation of a dipole-bound electron as the initial excited state. In the anionic cluster studies from the literature,[33,34] the dipole-bound electron was generated by pumping the chromophore with a photon of slightly more energy than the electron binding energy. However, in the experiments reported here, the excitation energy (9.0−9.4 eV) is somewhat less than the IP of the chromophore (12.35 eV). As a result, a somewhat different description of the CTTS process is presented here than was presented in the studies discussed above. This difference between the excitation energy and the IP of the chromophore is believed to be overcome by the electron affinity of the solvent molecules of the cluster. The vertical detachment energies of $(SO_2)_m^-$ clusters have been measured,[25] and it is assumed here that the electron affinity of the neutral cluster is approximately the same as this detachment energy of the anion. An energetics calculation of the CTTS process is shown in Table 5. It should be noted that the exact values of the binding energy between the SO_2^+ and the $(SO_2)_m^-$ clusters is not known, but it is expected to be substantially greater than the binding energy of the neutral species. As a result, the difference between the IP of SO_2 and the cluster vertical detachment energy (VDE) is the upper limit of the energy needed for the CTTS process to proceed. In other words, if the combination of the two-photon pump energy and the VDE of the cluster exceeds the IP of SO_2, CTTS can occur. To emphasize the strong correlation between the combined energy and the excited-state lifetime, the values in Table 4 are presented as a plot of combined energy as a function of the value of τ_2 in Figure 8. The best fit straight line shows the strong correlation to all cluster sizes except the $m = 1$ points (not included in the fit). Thus, it appears that only the $m = 1$ species has insufficient energy to undergo CTTS under the excitation energy used. The meaning of the fit line is not entirely clear. However, it seems reasonable to suspect that the intercept value of the line should be the minimum energy for the CTTS process to occur which would be the IP of the SO_2 chromophore. Therefore, the difference between the intercept and the IP is probably the combination of the energies that were not considered in the calculation such as the binding energy just discussed. So, the change in the binding energy from the molecular cluster to the CTTS cluster should be about 12.35 eV − 11.85 eV = 0.5 eV, which seems like a reasonable value.

At this point it is again pertinent to comment on the assumption discussed earlier, which asserted that an SO_2 molecule evaporates from each cluster during the ionization process. The correlation between the value of τ_2, the cluster size, and the pump energy is believed to be an indication of the CTTS process. Therefore, the observed dependence of the value of τ_2 on the excitation energy for the $m = 2$ cluster (Table 4), which is detected in the mass spectrum as SO_2SO^+, indicates that the neutral cluster that is detected as SO_2SO^+ is undergoing CTTS. However, according to the energy calculation shown in Table 5 and the VDE values tabulated in Table 4, it is not energetically possible, in the range of pump energies used, for a cluster smaller than the $(SO_2)_3$ to undergo CTTS. This is because at least two solvent molecules must be present in the cluster, in addition to the chromophore molecule (making the total cluster size three SO_2 molecules), for the excitation energy + electron affinity (VDE) to approach the IP of the SO_2 chromophore. Therefore, to account for the excitation energy dependence of τ_2 observed for the SO_2SO^+ signal, it must be assumed that an SO_2 molecule evaporated from the cluster following ionization along with the O atom loss, making $(SO_2)_3$ the neutral source of SO_2SO^+.

In light of the above discussion of CTTS energetics, the CTTS is not energetically feasible in the $m = 1$ cluster; another process must be occurring within this cluster to account for the observed dynamics. However, a clear source of the dynamics cannot be identified. It may be that the signal of $m = 1$ species is a combination of signals from several neutral sources such as SO_2 molecules that did not form clusters in the source, $(SO_2)_2$ clusters, and fragmentation of other clusters that were not stable enough to be detected intact.

4.3.5. Interpretation of Time Constant, τ_2. As discussed above, the cluster size dependence of τ_2 correlates well with the CTTS mechanism proposed here. However, the exact nature of the relaxation process associated with τ_2 is difficult to identify with the experiment performed here, but some possibilities have been proposed in the CTTS literature, including the following mechanisms. Recombination of the electron with the chromophore molecule has been reported for a solution-phase experiment, but recombination occurs on the time scale of hundreds of picoseconds[36,38] and is therefore not likely to be the source of the observed decay. Also, it is believed that recombination would release so much energy that, in the case of a cluster, extensive fragmentation would occur and metastable decay peaks would be observed in the mass spectrum.[33] Thermionic emission has also been proposed in the case of anion clusters due to the fact that the chromophore has been excited beyond its ionization potential.[33] However, this argument does not apply in the case of the neutral clusters being studied, as is explained shortly. Another possible explanation would be evaporation of a single molecule due to the energy transfer from the electron to the cluster. However, one would expect to see slow growth in the smaller clusters on the time scale of the decay of the larger ones; however, this is not observed. In fact, the smaller clusters have a faster decay than the larger ones, eliminating the possibility of an evaporation mechanism.

The final and perhaps most likely explanation for τ_2 is that as the energy of the electronic excitation is transferred to the cluster, the energy of the remaining electronic excitation subsequently decreases, resulting in an increase in the energy needed to promote an electron to above the ionization potential of the cluster. Once the energy needed exceeds the energy of

one probe photon, the ionization efficiency is expected to drop and the signal intensity decrease. This interpretation agrees with the observed results for two reasons. First, the absorption cross-section for the excited state that produces τ_1 and τ_2 is poor, as evidenced by the data in Figure 5A, where it can be seen that at the low end of the range of probe pulse energies used, the signal intensity produced from the one-photon probe of the F band excitation is of about the same intensity as the signal from the $^1A_2$ and $^1B_1$ states, which requires the absorption of three photons. Therefore, once the absorption of a second photon was needed to produce the τ_2 component, ionization would become unlikely. Second, the interpretation agrees with the observed cluster size and wavelength effects on the value of τ_2. Larger clusters have lower IP's as indicated by the REMPI measurement of SO_2 (12.348 eV) and $(SO_2)_2$ (11.72 eV).[4] Thus, as the cluster gets larger, the electron would have to dissipate more energy to get to ~3 eV below the IP in a larger cluster, which would take more time. Also, when a shorter wavelength was used, the electron has more energy to dissipate, which will also take more time.

4.4. Proposed Sources of Oxygen Atom Loss. With the above observations relating to CTTS in mind, this discussion now returns to the source of the oxygen loss that leads to the observation of clusters with two or (depending on the identity of *m*/*z* 80 and *m*/*z* 144, as mentioned in the Results) possibly three fewer oxygen atoms than the original neutral cluster. One key observation that can be seen from the data presented in Table 3 is that the value of τ_2 is dependent on the number of oxygen atoms lost, with τ_2 decreasing as the number of oxygen atoms lost increases. This leads one to suspect that a neutral-state process is involved in their formation. The other key observation is that the same cluster distribution is observed under the conditions of a pump−probe experiment where two laser pulses are interacting with the cluster beam and under conditions of multiphoton ionization by 400 nm light[40] from a single laser pulse. This leads one to suspect that the oxygen loss occurs following the formation of the cationic cluster, which has been observed for SO_2^+, as discussed earlier. However, if the oxygen loss process occurs entirely in the ion state, each of the cluster fragments must display the same dynamic behavior because the temporal measurement in a pump−probe experiment occurs before the ionization event. To reconcile these two seemingly conflicting points, one indicating that the oxygen loss must occur in the ion state and the other indicating that it must involve a neutral cluster process, an oxygen loss mechanism must exist that can occur in either the cationic or neutral state and produce the same products. This may not be as unlikely as it sounds. According to the CTTS mechanism proposed above for neutral SO_2 clusters of $m > 1$, the products of CTTS are $SO_2^+ \cdot (SO_2)_m^-$. As mentioned, SO_2^+ is known to undergo oxygen loss and therefore could do so in the CTTS cluster prior to ionization. This would undoubtedly influence the measured value of τ_2 because the oxygen loss would involve the dissipation or transfer of energy, the process that is believed to lead to the decay represented by τ_2. Also, because fragmentation of SO_2^+ is occurring in both mechanisms, the same products should be observed for the fragmentation in the neutral cluster that underwent CTTS, as is observed following direct ionization. Thus, this mechanism resolves the apparent conflicting observation of the fragments present under conditions of direct ionization and in the pump−probe experiment. Some confirmation of this mechanism can be found in a publication of an SO_2 cluster pump−probe experiment performed at a lower excitation energy where the dynamics of the $(SO_2)_m^+$ and $(SO_2)_{m-1}SO^+$ clusters were found to have the same time constants. These findings indicate that in this instance, the loss of the oxygen atom indeed occurred in the ion state.[11] As just discussed, the CTTS mechanism may be involved in the formation of oxygen deficient clusters observed in the mass spectrum. However, it is difficult to explain the loss of three oxygen atoms from the cluster with CTTS. Therefore, the identity and source of the *m*/*z* 80 and *m*/*z* 144 clusters remains uncertain.

5. Conclusions

The excited-state dynamics of $(SO_2)_m$ clusters following excitation by ultrafast laser pulses in the range of 4.5 eV (coupled $^1A_2$ and $^1B_1$ states) and 9 eV (F band) have been investigated. The findings for the coupled $^1A_2$ and $^1B_1$ states are in good agreement with published computational work on the properties of these coupled states. In addition, some possible sources of the observed trends in the measured lifetimes associated with these states have been proposed. A mechanism involving charge transfer to solvent has been put forward as the source of the excited-state dynamics that follow the excitation of the SO_2 F band within $(SO_2)_{m+1}$ clusters with $m > 1$. The CTTS mechanism has been supported by calculations of the energetics of the process and the observed trends in the excited-state lifetimes that correlate very well with the calculated energies.

As future studies continue the investigation of systems similar to those studied here, trends in the results will inevitably clarify many of the proposed mechanisms discussed. In terms of the SO_2 CTTS process, which is apparently mediated by the high electron affinity of SO_2 clusters, studies using other high electron affinity solvents may aid in verifying the proposed mechanism. This verification is of particularly significant because, as far as can be determined from the literature, CTTS has not been previously reported in a neutral cluster system. Therefore, the properties of this mechanism cannot be confirmed by comparison to other neutral cluster systems until such experiments have been performed.

Acknowledgment. Financial support by the Atmospheric Sciences and Experimental Physical Chemistry Divisions of the U.S. National Science Foundation, Grant No. ATM-0411954, is gratefully acknowledged.

References and Notes

(1) Hewitt, C. N. *Atmos. Environ.* **2001**, *35*, 1155.
(2) Abbatt, J. D. P. *Chem. Rev.* **2003**, *103*, 4783.
(3) Xue, B.; Chen, Y.; Hai-Lung Dai. *J. Chem. Phys.* **2000**, *112*, 2210.
(4) Erickson, J.; Ng C. Y. *J. Chem. Phys.* **1981**, *75*, 1650.
(5) Muller, H.; Koppel, H. *Chem. Phys.* **1994**, *183*, 107.
(6) Kamaya, K.; Matsui, H. *Bull. Chem. Soc. Jpn.* **1991**, *64*, 2792.
(7) Katagiri, H.; Sako, T.; Hishikawa, A.; Yazaki, T.; Onda, K.; Yamanouchi, K.; Yoshino, K. *J. Mol. Struct.* **1997**, *413*, 589.
(8) Zewail, A. H. *Science* **1988**, *242*, 1645.
(9) Zewail, A. H. *J. Phys. Chem. A* **2000**, *104*, 5660.
(10) Knapenberger, K. L., Jr.; Castleman, A. W., Jr. *J. Phys. Chem. A* **2004**, *108*, 9.
(11) Knappenberger, K. L., Jr.; Castleman, A. W., Jr. *J. Chem. Phys.* **2004**, *121*, 3540.
(12) Hurley, S. M.; Dermota, T. E.; Hydutsky, D. P.; Castleman, A. W., Jr. *J. Phys. Chem. A* **2003**, *107*, 3497.
(13) Bergmann, T.; Martin, T. P.; Schaber, H. *Rev. Sci. Instrum.* **1990**, *61*, 2592.
(14) Wiley, W. C.; McLaren, I. H. *Rev. Sci. Instrum.* **1955**, *26*, 1150.
(15) Spectra Physics, 1335 Terra Bella Ave, Mountain View, CA 94039.
(16) General Valve, Parker Hannifin Corp., 19 Gloria Lane, Fairfield NJ 07004.
(17) Burle Electrooptics, Sturbridge Business Park, P.O. Box 1159, Sturbridge, MA 01566.
(18) LeCroy Corp., 690 Chestnut Ridge Rd, Chestnut Ridge, NY 10977.
(19) Aerotech, Inc., 101 Zeta Dr., Pittsburgh, PA 15238-2897.

(20) National Instruments Corp., 11500 N. Mopac Expwy, Austin, TX 78759-3504.
(21) Pedersen, S.; Zewail, A. H. *Mol. Phys.* **1996**, *89*, 1455.
(22) Fiebig, T.; Chachisvilis, M.; Manger, M.; Zewail, A. H.; Douhal, A.; Garcia-Ochoa, I.; De La Hoz Ayuso, A. *J. Phys. Chem. A* **1999**, *103*, 7419.
(23) Oakdale Engineering, 23 Tomey Rd, Oakdale, PA 15071.
(24) Bone, R. G. A.; Le Sueur, C. R.; Amos, R. D.; Stone, A. J. *J. Chem. Phys* **1992**, *96*, 8390.
(25) Tsukuda, T.; Hirose, T.; Nagata T. *Int. J. Mass Spectrom.* **1997**, *171*, 273.
(26) Zhang, L.; Pei, L.; Dai, J.; Zhang, T.; Chen, C.; Yu, S.; Ma, X. *Chem. Phys. Lett.* **1996**, *259*, 403.
(27) Thomas, T. F.; Dale, F.; Paulson, J. F. *J. Chem. Phys.* **1986**, *84*, 1215.
(28) Snodgrass, J. T.; Bunn, T. L.; Bowers M. T. *Int. J. Mass. Spectrom.* **1990**, *102*, 45.
(29) Okabe, H. *Photochemistry of Small Molecules*; Wiley: New York, 1978; p 252.
(30) Vuskovic, L.; Trajmar, S. *J. Chem. Phys.* **1982**, *77*, 5436.
(31) Dastareer, A.; Hegazi, E.; Hamdan, A.; Al-Adel, F. *Chem. Phys. Lett.* **1997**, *275*, 283.
(32) Dermota, T. E.; Zhong, Q.; Castleman, A. W., Jr. *Chem. Rev.* **2004**, *104*, 1861.
(33) Davis, A. V.; Zanni, M. T.; Frischkorn, C.; Neumark, D. M. *J. Electron. Spectrosc.* **2000**, *108*, 203.
(34) Davis, A. V.; Zanni, M. T.; Weinkauf, R.; Neumark, D. M. *Chem. Phys. Lett.* **2002**, *353*, 455.
(35) Sheu, W. S.; Liu, Y. T. *Chem. Phys. Lett.* **2003**, *374*, 620.
(36) Barthel, E. R.; Martini, I. B.; Schwartz, B. J. *J. Phys. Chem. B* **2001**, *105*, 12230.
(37) Barthel, E. R.; Martini, I. B.; Keszei, E.; Schwartz, B. J. *J. Chem. Phys.* **2003**, *118*, 5916.
(38) Kloepfer, J. A.; Vilchiz, V. H.; Lenchenkov, V. A.; Gernaine, A. C.; Bradforth, S. E. *J. Chem. Phys.* **2000**, *113*, 6288.
(39) Assel, M.; Laenen, R.; Laubereau, A. *Chem. Phys. Lett.* **1998**, *289*, 267.
(40) Zhong, Q.; Hurley, S. M.; Castleman, A. W., Jr. *Int. J. Mass Spectrom.* **1999**, *185*, 905.
(41) Watkins, I. W. *J. Mol. Spectrosc.* **1969**, *29*, 402..
(42) Hurley, S. M.; Dermota, T. E.; Hydutsky, D. P.; Castleman, A. W., Jr. *Science* **2002**, *298*, 202.
(43) Hurley, S. M.; Dermota, T. E.; Hydutsky, D. P.; Castleman, A. W., Jr. *J. Chem. Phys.* **2003**, *118*, 9272.